Article ID: 1006-8775(2024)01-0020-09

An Evaluation of Tropical Cyclone Genesis Forecast over the Western North Pacific and the South China Sea from the CMA-TRAMS

LI Meng-jie (李梦婕)[1,2], CHEN Zi-tong (陈子通)[1], DAI Guang-feng (戴光丰)[1], TIAN Qun (田 群)[1], LEUNG Jeremy Cheuk-hin (梁卓轩)[1], LIN Qing (林 青)[3], ZHANG Yan-xia (张艳霞)[1,2]

(1. Guangzhou Institute of Tropical and Marine Meteorology/ Guangdong Provincial Key Laboratory of Regional Numerical Weather Prediction, CMA, Guangzhou 510641 China; 2. State Key Laboratory of Severe Weather, Chinese Academy of Meteorological Sciences, Beijing 100081 China; 3. Guangdong Meteorological Observatory, Guangzhou 510641 China)

Abstract: Tropical cyclone (TC) genesis forecasting is essential for daily operational practices during the typhoon season. The updated version of the Tropical Regional Atmosphere Model for the South China Sea (CMA-TRAMS) offers forecasters reliable numerical weather prediction (NWP) products with improved configurations and fine resolution. While traditional evaluation of typhoon forecasts has focused on track and intensity, the increasing accuracy of TC genesis forecasts calls for more comprehensive evaluation methods to assess the reliability of these predictions. This study aims to evaluate the effectiveness of the CMA-TRAMS for cyclogenesis forecasts over the western North Pacific and South China Sea. Based on previous research and typhoon observation data over five years, a set of localized, objective criteria has been proposed. The analysis results indicate that the CMA-TRAMS demonstrated superiority in cyclogenesis forecasts, predicting 6 out of 22 TCs with a forecast lead time of up to 144 h. Additionally, over 80% of the total could be predicted 72 h in advance. The model also showed an average TC genesis position error of 218.3 km, comparable to the track errors of operational models according to the annual evaluation. The study also briefly investigated the forecast of Noul (2011). The forecast field of the CMA-TRAMS depicted thermal and dynamical conditions that could trigger typhoon genesis, consistent with the analysis field. The 96-hour forecast field of the CMA-TRAMS displayed a relatively organized three-dimensional structure of the typhoon. These results can enhance understanding of the mechanism behind typhoon genesis, fine-tune model configurations and dynamical frameworks, and provide reliable forecasts for forecasters.

Key words: CMA-TRAMS; cyclogenesis; numerical weather prediction; tropical cyclone

CLC number: P45 **Document code:** A

Citation: LI Meng-jie, CHEN Zi-tong, DAI Guang-feng, et al. An Evaluation of Tropical Cyclone Genesis Forecast over the Western North Pacific and the South China Sea from the CMA-TRAMS [J]. Journal of Tropical Meteorology, 2024, 30 (1): 20-28, https://doi.org/10.3724/j.1006-8775.2024.003

1 INTRODUCTION

As one of the critical issues in tropical cyclone (TC) research, the TC genesis problem has recently attracted considerable attention from scientists. The TC genesis is recognized as continuous interactions of dynamic and thermodynamic processes at multi-scales (Tang et al. [1]), and various oceanic and atmospheric factors determine whether and how tropical disturbances develop into TCs (Zhang et al. [2]). The conditional instability of the second kind (CISK; Charney and Eliassen [3]) and wind-induced surface heat exchange (WISHE; Emanuel [4]) are the classic theory of typhoon genesis. Bottom-up (Montgomery and Enagonio [5]; Montgomery et al. [6]), top-down (Ritchie and Holland [7]; Simpson et al. [8]), pouch (Dunkerto et al. [9]) and other hypotheses have been subsequently proposed. Due to the complex mechanism of TC generation and the scarcity of offshore observations, this problem has become the most challenging topic in TC research. Although the mechanism of typhoon generation is not fully understood, numerical models are not constrained by these genesis theories or necessary conditions; therefore, they can predict the development beyond those physically accepted causes (Halperin et al. [10]). However, models will still be limited by resolution, computational efficiency, etc, so one cannot expect the models to fully resolve all the processes required for TC generation.

Assessing the forecasting skill of models is necessary. Currently, the measurements of TC track and intensity have been well established, and every year many institutions and researchers conduct annual assessments of the predictive capability of global (Yamaguchi et al. [11]; Chen et al. [12]; Chen et al. [13]) and regional (Das et al. [14]; Chen et al. [15, 16]) models. In contrast to a large number of research on TC track and intensity forecast capability, the amount of literature on the predictability of typhoon

Received 2023-10-25; **Revised** 2023-11-15; **Accepted** 2024-02-15

Funding: Science and Technology Innovation Project of Guangdong Provincial Water Resources Department (2022-01); Science and Technology Program of Guangdong Province (2022A1515011870); China Meteorological Administration Key Innovation Team of Tropical Meteorology (CMA2023ZD08); Open Research Program of the State Key Laboratory of Severe Weather (2022LASW-B18)

Biography: LI Meng-jie, primarily undertaking research on numerical weather prediction.

Corresponding author: CHEN Zi-tong, e-mail: chenzt@gd121.cn

genesis by models is relatively small. Several studies have investigated global models' ability to predict TC genesis in mostly, the eastern North Pacific (EPAC) basins and the North Atlantic (NATL) basin. Pasch et al. [17] analyzed the performance of three global models (GFS, NOGAPS, and UKMET) in predicting TC genesis during the 2005 Atlantic hurricane season, indicating that global models provided quite reliable guidance for the prediction of TC formation. Halperin et al. have set a series of experiments to assess the improvement or degradation of global models from three aspects: temporal, spatial, and model configuration [10, 18, 19]. The research above mainly focused on global models over the EPAC basin or the NATL basin. Currently, it is urged to access the capability of regional models for forecasting cyclogenesis in the western North Pacific and the South China Sea. This is the area with the highest frequency of TCs globally (Chen et al. [20]). Because of its geographical location and long coastline, China is one of the countries most severely affected by typhoons in the world (Zhang et al. [21]). China Meteorological Administration Tropical Regional Atmosphere Model for the South China Sea (CMA-TRAMS) is developed based on the GRAPES regional model (Chen et al. [22]). Since 2004, Guangzhou Institute of Tropical and Marine Meteorology of China Meteorological Administration (ITMM, CMA) has developed a numerical weather prediction system for tropical region based on GRAPES and the self-developed TL model (Tropical Limited Zone Model) which is the predecessors of CMA-TRAMS (Chen et al. [23]). Its primary purpose is to provide typhoon numerical forecast products for the South China Sea. After a period of development, the track and intensity forecasting skills of the CMA-TRAMS have improved (Chen et al. [24]; Xu et al. [25]) and are favored by forecasters.

The purpose of this work is three folds: (1) To establish a set of preliminary objective criteria based on observation data and previous research results. (2) To evaluate the performance of CMA-TRAMS in forecasting the genesis of typhoons during 2020. (3) To examine the thermal and dynamic conditions in the CMA-TRAMS forecast by exploring the case of Typhoon Noul. The following section details the methods, including the CMA-TRAMS configurations and the criteria utilized to identify a cyclogenesis event. Section 3 presents the analysis results and a brief case study on the cyclogenesis forecast for Noul (2011). A summary and prospects are provided in Section 4.

2 METHODOLOGY

2.1 *Model configuration*

Since its origin, the CMA-TRAMS has undergone three upgrades. In 2019, the CMA-TRAMS has gone through its latest upgrade to version 3.0 (V3.0), which includes: model resolution, dynamic framework, and physical process. The fundamental features of the CMA-TRAMS V3.0 dynamical framework are the same as those of the CMA-TRAMS V2.0, maintaining GRAPES fully compressible-nonhydrostatic equilibrium, semi-implicit-semi-Lagrangian (SISL), static reference atmosphere, altitude terrain-following coordinates, Charney-Philips vertical jump, horizontal equidistance longitude-latitude grid, and Arakawa-C jump. The scheme of boundary layer parameterization and the scheme of gravity wave drag from sub-grid scale orography are also the same as CMA-TRAMS V2.0. CMA-TRAMS V3.0 has updated the microphysical WSM6 scheme, which introduces the latest new deep convection parameterization scheme. The sea-land surface parameterization makes some optimizations based on the original scheme and it adds land surface analysis to improve the accuracy of land surface forecast. For short and long-wave radiation, the original RRTM has been upgraded to RRTMG. CMA-TRAMS V3.0 has improved the high-resolution dynamical framework based on the 3D reference atmosphere, introduced a new horizontal diffusion scheme, improved the Lagrangian advection algorithm, and further developed the iterative method SISL technical scheme. Meanwhile, the CMA-TRAMS V3.0 has optimized the invocation method and technical parameters of each physical process block of the model. Other physical process schemes used in the CMA-TRAMS V3.0 include WSM6 microphysical process, NSAS convection parameterization, NMRF boundary layer parameterization, SMS land surface process, SFCALY near-surface scheme, and RRTMG long- and short-wave radiation scheme [8] (further explanation of the CMA-TRAMS V 3.0 can be seen in the paper of Chen et al. [24], and Xu et al. [25]).

The new version of the model covers 70°–160°E, 0.8°–54.8°N, with a resolution of 9 km, 65-layer topographic follow-up coordinates in the vertical direction, and a model top height of 31 km. The model generates the initial and lateral boundary conditions with the analysis and forecast fields provided by the European Center of Median Weather Forecasts - Integrated Forecast System (ECMWF-IFS) [26] with a resolution of 0.125°. The model runs twice a day (at 0000 and 1200 UTC), with forwarding integration of 168 h each time.

2.2 *Definition of cyclogenesis criteria*

The TC observation data we use in this study is taken from the China Meteorological Administration typhoon website (http://www.typhoon.org.cn/). TC genesis is defined as the first time when CMA designates a cyclone as a tropical depression (TD) or tropical storm (TS). Since the model is activated twice a day, for statistical convenience, we have unified TC genesis time to either 0000 UTC or 1200 UTC, whichever is the nearest moment of its generation.

The criteria for typhoon generation have been defined in some references. In 1975, Gray [27] summarized six primary genesis parameters in the western North Pacific which were: low-level relative vorticity, Coriolis parameter, vertical wind shear from lower to upper troposphere, ocean thermal condition, vertical gradient θ_e

between surface and 500hPa, and middle troposphere relative humidity. The criteria employed in this study partially relied on Daniel's finding in 2016 [19]. Firstly, in order to identify a TC, a point of relative minimum mean sea level pressure (MLSP) must be located, a maximum relative vortex at 850 height and a maximum thickness of 200–850 hPa should be found within a 2-degree radius of the point. Additionally, the maximum wind speed of 925 hPa must exceed the threshold within 5 degrees of the minimum MLSP point. To meet the time threshold, these criteria must be forecasted continuously for at least 24 h.

Considering the differences in generating basin (Daniel discussed TC genesis forecasts over the NATL and eastern North Pacific with North Atlantic basins mainly), we collected basic information on TCs generated over the western North Pacific and South China Sea from 2015 to 2019, including details on onset time, location, and generation intensity, as presented in Fig. 1. Based on this data, a set of localized objective criteria with specific thresholds were established. Moreover, considering future operational requirements, the variables selected should be convenient to obtain and calculate. Following are the preliminary recognizing criteria and thresholds that we employed in this paper:

(1) The minimum MSLP must be lower than 1005 hPa;

(2) The sea surface temperature (SST) of the nearby sea area must be higher than 26 °C;

(3) The maximum wind must be greater than 10.8 m s^{-1};

(4) The land-sea ratio around the minimum MSLP (5 grids in this article) must be greater than 0.8;

(5) The pressure gradient must be greater than 0.1 hPa km^{-1}.

For a double check, the identified vortexes must be predicted at two consecutive forecast initial times.

As Halperin explained, criteria 1–3 are consistent with the primary meteorological conditions during the formation of TCs. Criterion 4 attempts to avoid misjudgment of low pressure on the land surface. Criterion 5 is hired to confirm the closure of isobar [10]. Since the system will return a few vortexes each time, care must be taken to ensure that the identified vortex is not a similar TC nor a passing listed TC, but a truly TC that will occur in a few days. Therefore, to avoid false alarms, a final check is included - a vortex meeting the above criteria must be forecasted for two consecutive initial times.

3 VERIFICATION OF TC GENESIS FORECAST

3.1 *Statistical analysis*

A total of 23 named TCs have formed over the western North Pacific and the South China Sea in 2020. However, Typhoon Kujira (2013) was not included in this paper since it was close to the side boundary of the regional model, making the model unable to predict its genesis. Therefore, there were 22 valid cases in this paper. The performance of the model-indicated cyclogenesis was assessed from two aspects, forecast length and position error. This paper mainly evaluated the forecast results from the CMA-TRAMS and ECMWF.

The comparison of the earliest predicted time for TC genesis between the ECMWF and CMA-TRAMS is shown in Fig. 2. Both models had the capability of predicting the formation of typhoons, with a maximum lead time of 144 h. Six TCs could be predicted 144 h in advance by the CMA-TRAMS, while 18 TCs were predicted 3 days in advance, and there were no missing events - meaning all TCs had been forecasted at least 24 h in advance. The ECMWF had only one hit 144 h in advance, and 8 hits 72 h in advance. The ECMWF missed the genesis of Hagupit (2004) and Goni (2019), even 24 h before the event, there was no vortex forecasted over the basin. The average genesis forecast lead time was 84 h by the CMA-TRAMS, compared to 48 h by the ECMWF.

The comparison of position errors in cyclogenesis between two models is shown in Fig. 3. The shading depicts the forecast error range for various lead times, while the curved lines indicate the mean forecast errors for each lead times. As expected, the model performance decreased as forecast lead time increased. For lead times of 24 h, 48 h, and 72 h, the mean genesis position errors of the CMA-TRAMS were 99.84 km, 158.13 km, and 218.3 km, respectively, while the mean errors of the ECMWF were 108.25 km, 173.75 km, and 214.6 km,

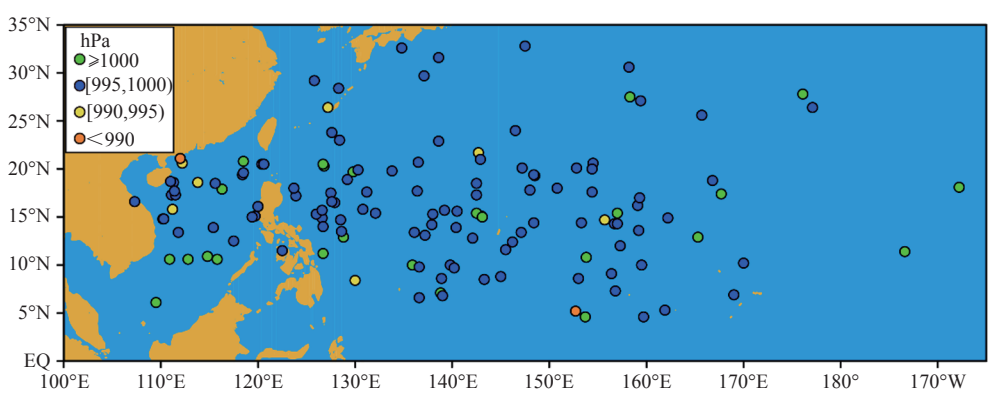

Figure 1. A geographic plot of observed TC genesis events over the western North Pacific and South China Sea from 2015 to 2019. The genesis intensity (the minimum MSLP: hPa) of each event is indicated by different colors.

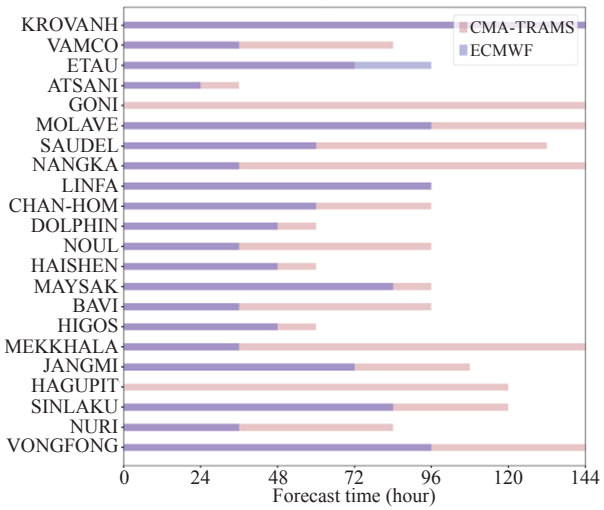

Figure 2. The maximum forecast lead time of TC genesis events in 2020 for the CMA-TRAMS (red) and ECMWF (blue). The vertical coordinate is the name of each TC that formed in 2020.

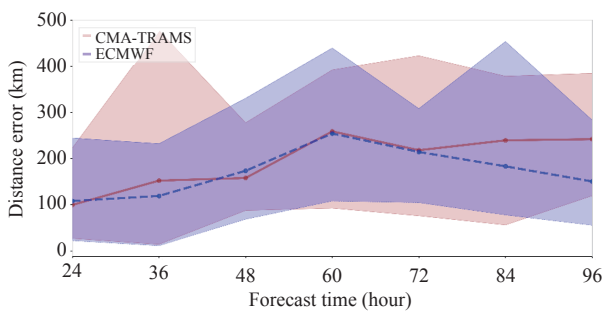

Figure 3. Common comparison of mean genesis position errors (km) along with different forecast lead times for the CMA-TRAMS (red) and ECMWF (blue). The error ranges for each model are indicated by the same transparent color shadings.

respectively. Within the lead time of 72 h, although the CMA-TRAMS exhibited a large error range on individual cases, the mean genesis position errors of these two models were basically the same, with the CMA-TRAMS performing slightly better than the ECMWF.

Shanghai Typhoon Institute, STI/CMA conducts the annual verification and analyses on operational forecasts of TCs over the western North Pacific and the South China Sea every year, which include assessments of the track and intensity errors for both global models and regional models. Twenty-three named typhoons over the western North Pacific and the South China Sea in 2020 were evaluated by Chen et al. [16]. In the study, four global models were the National Centers for Environmental Prediction Global Forecast System (NCEP-GFS), the ECMWF-IFS, the United Kingdom Meteorological Office Unified Model (UKMO-MetUM), and the Japan Meteorological Agency's Global Spectral Model (JMA-GSM); four regional models were the CMA-TRAMS, the CMA-Typhoon Model (CMA-TYM), the CMA-Tropical Cyclone Model (CMA-TCM) and the Hurricane Weather Research and Forecasting model (HWRF). Table 1 shows

Table 1. Comparison of mean TC track forecast error (km) and mean TC genesis position forecast error (km) along with different forecast lead times in 2020.

Model	24h	48h	72h
Global Model	66.6	117.8	187.3
Regional Model	77.85	152.275	216.875
CMA-TRAMS	61.3	116.8	173.4
CMA-TRAMS (genesis)	99.84	158.13	218.3

that the mean 72 h track error of the CMA-TRAMS in 2020 was 173.4 km, the smallest among both global and regional models. The 72 h track errors for several models exceed 200 km, while the 72 h genesis position error for the CMA-TRAMS was 218.3 km. This suggested that the 72 h genesis position forecast of the CMA-TRAMS was comparable to the 72 h track forecast of other models.

3.2 *Case study*

Compared to the western North Pacific formed TCs, TCs over the South China Sea have characteristics including smaller circulation structure, shorter life cycle, asymmetrical shape, and complex track, making it a key and difficult issue for coastal countries to forecast [28,29].

Typhoon Noul, the 11th typhoon of 2020 formed from a low-pressure area that began on the eastern side of the Philippines and became a TD on 15 September. Typhoon Noul had taken on a general northwestward motion while steadily its way across the South China Sea. Typhoon Noul had strengthened to the level of severe TS and finally made its landfall in Vietnam on 18 September. Due to Noul, strong winds and heavy rainstorms had affected the cities along the coastline.

Using the criteria introduced above, the cyclone genesis position at different initial forecast times from 0000 UTC 12 September to 1000 UTC 15 September was determined. As shown in Fig. 4, the CMA-TRAMS provided a maximum forecast lead time of 96 h, which was significantly longer than that of the ECMWF (36 h in advance). The CMA-TRAMS showed a larger deviation in the forecast onset position compared to the ECMWF, despite its longer lead time in forecasting typhoon genesis. As the forecast time gradually approached the genesis time, the forecasts of cyclogenesis position by both models were getting closer to the observed position. According to Table 2, 24 h before the genesis event, the ECMWF's forecast result was closer to the observed position than the CMA-TRAMS's, with distance errors of 31.03 km and 124.67 km, respectively. This case was consistent with the conclusions of the previous section.

Figure 5 shows the distribution of simulated TC tracks at different initial times. The observed track of Noul was not complex, both models could capture its northwestward motion. The CMA-TRAMS initialized at 0000 UTC 12 September was the first time when Noul was detected. Although the forecasted typhoon moved steadily ahead its way across the South China Sea along the observed track, there in fact quite a lag existed.

In general, both models had good performances in this

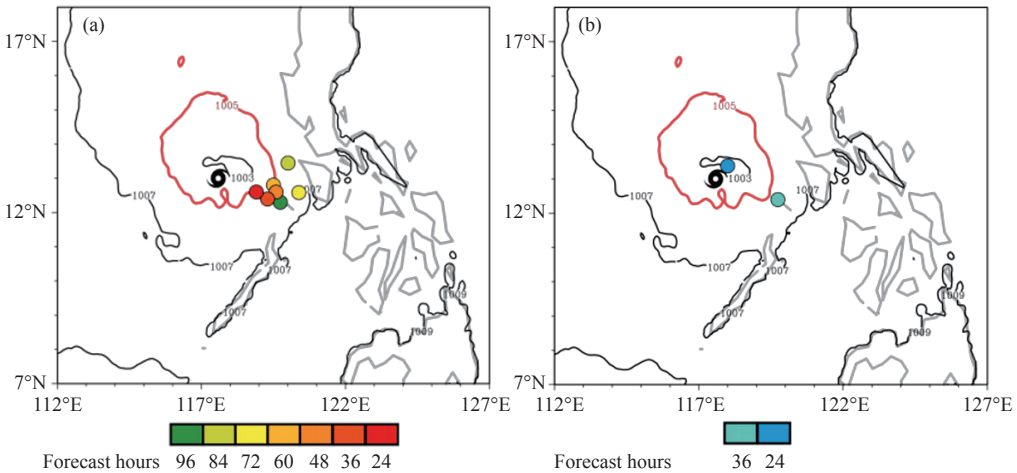

Figure 4. Spatial distribution of TC genesis position of different forecast lead times. (a) CMA-TRAMS, and (b) ECMWF.

Table 2. Genesis position forecast error of each model (km).

Leading hours (h)	CMA-TRAMS	ECMWF
24	124.67	31.03
36	185.83	224.55
48	205.38	/
60	164.78	/
72	272.46	/
84	227.4	/
96	234.22	/

Table 3. Track error and intensity error of each model.

Forecast length (h)	Track error (km)		Intensity error (hPa)	
	ECMWF	CMA-TRAMS	ECMWF	CMA-TRAMS
6	49.2	50.7	3.9	2.3
12	53.4	56.3	4.6	3.3
18	80.3	61.1	5.2	4
24	105.9	88.6	5.5	4.7
30	118.7	103.2	3.4	5.1
36	129.6	122.6	5.1	9.4
42	122.5	131.4	3.8	7.2
48	77.6	116.6	4.8	7.8

case. For the track forecast, CMA-TRAMS and ECMWF exhibited comparable forecasting ability. The intensity forecast of ECMWF was more stable and accurate; while the intensity error of CMA-TRAMS increased as the forecast time extended (Table 3).

Over the main TCs genesis basin, high sea surface temperature (SST) and high humidity will make local convection easily activated, and this provides favorable conditions for TCs genesis. Fig. 6 (a) is the analysis data of the SST field at 0000 UTC 16 September 2020, and Fig. 6 (b, c) are the 96 h (4-day) forecast fields (initialized at 0000 UTC 12 September) of CMA-TRAMS and ECMWF, respectively. “Noul” formed in September, and the overall SST in the South China Sea was high, making it an ideal breeding basin for TC generation. In this case, the 4-day forecasts of both models had warm SST (> 26.5 °C) over the TC onset areas, but the environmental fields had distinct features in these two models. Despite a more accurate description of SST, ECMWF was unable to forecast this low-pressure center, and its 10m wind field was relatively weaker than the analysis field. Compared to the analysis, the CMA-TRAMS forecasted denser isobars (minimum SLP drop to 995 hPa) and stronger wind speeds around the typhoon center, but limited by the relatively small size of the high SST area, the circulation in the forecast appeared to be more compact, with some noise in the surrounding area. Anyway, SST in the western North

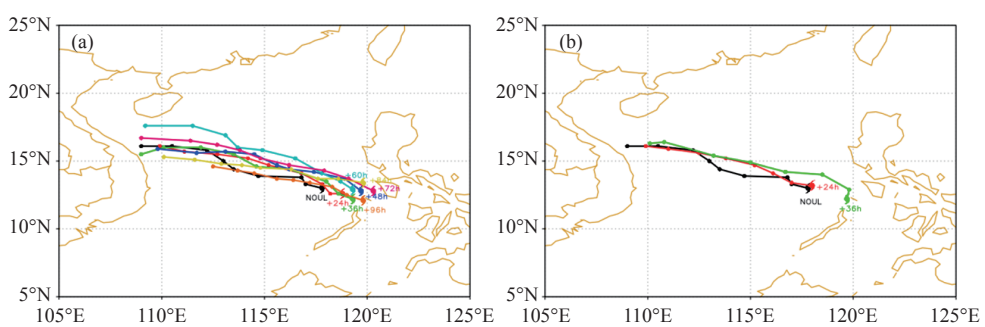

Figure 5. The observed track of typhoon Noul (black line) and the distribution of forecasted TC genesis positions and tracks of different forecast lead times (colored lines) from the (a) CMA-TRAMS and (b) ECMWF.

Pacific and the South China Sea during September provides ideal conditions for the cyclogenesis.

According to Fig. 7, the 4-day forecasts from both models had a high relative humidity (RH) in the lower atmosphere (at 925 hPa). The moisture content of the CMA-TRAMS had increased around the typhoon centre due to the genesis of the TC, while the surrounding area had a RH lower than 70%, this forecast result was very similar to the analysis field, meanwhile, compared to the analysis field, the ECMWF showed no obvious water vapor convergence. Up to 850 hPa height, the water vapor convergence remained pronounced, and the values slightly decreased in the analysis field. A similar water condition could be observed in the CMA-TRAMS, where the relative humidity exceeded 85%. However, in the ECMWF's forecasting a decrease in relative humidity, down to 80–85%, was observed. High relative humidity in the middle atmosphere was essential for typhoon development [30]. The large-scale circulation adjustment leads to a significant increase in water vapor transport and

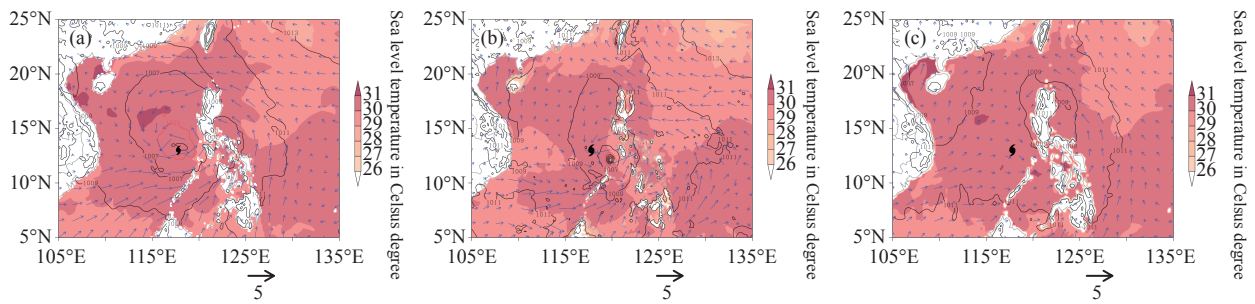

Figure 6. The sea surface temperature (°C; shadings), sea level pressure (hPa; contours), and 10m wind (m s^{-1}; vectors) from the (a) analysis data, (b) CMA-TRAMS forecast result initialized at 0000 UTC 12 September, and (c) ECMWF forecast result initialized at 0000 UTC 12 September.

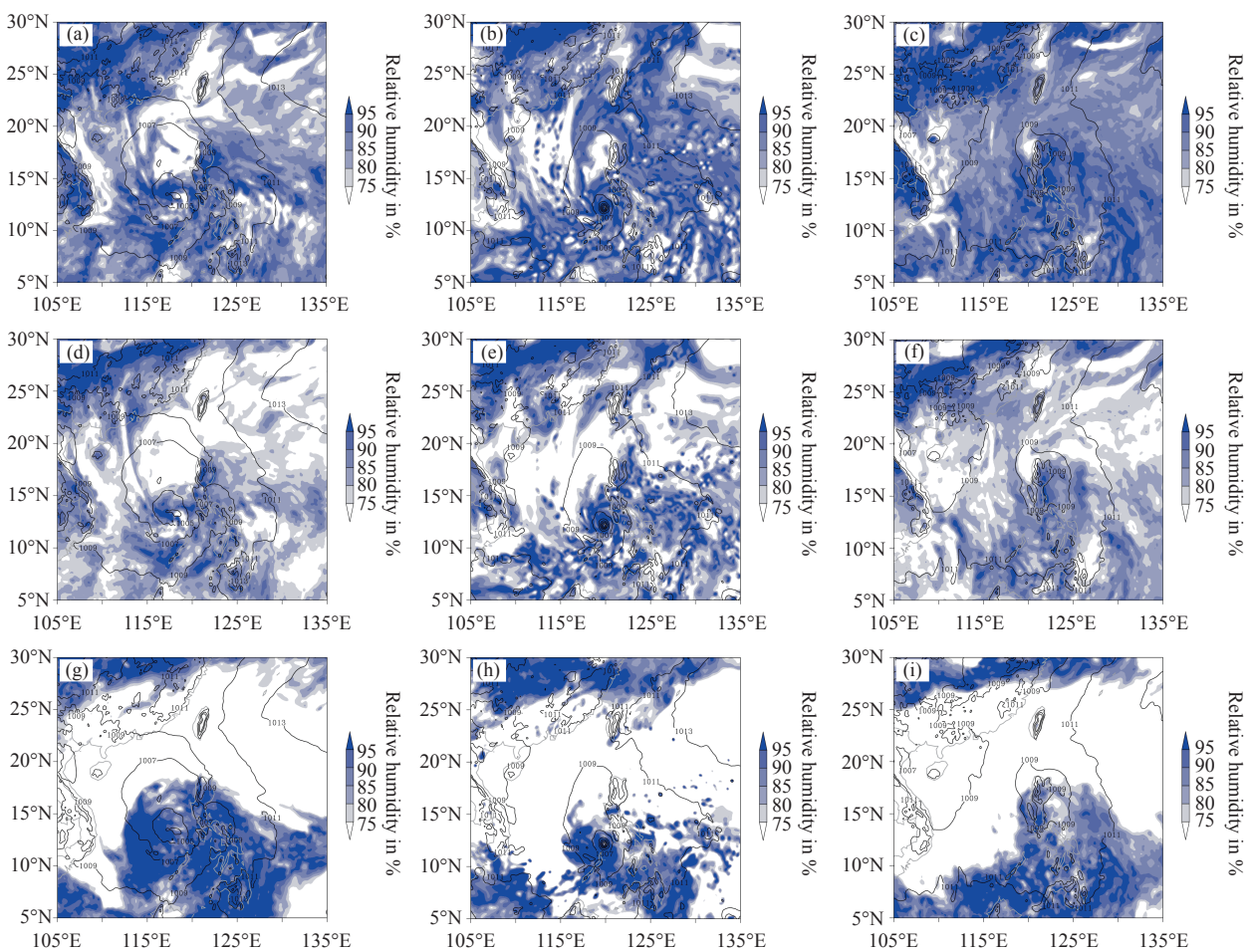

Figure 7. The relative humidity (%; shadings), sea level pressure (hPa; contours) from the (a, d, g) analysis field at 0000 UTC 16 September, (b, e, h) CMA-TRAMS forecast results initialized at 0000 UTC 12 September, and (c, f, i) ECMWF forecast results initialized at 0000 UTC 12 September. (a, b, c) present RH at 925hPa, (d, e, f) at 850 hPa, and (g, h, i) at 500 hPa.

the relative humidity in the mid- and upper-level of the typhoon, which facilitates the development of convection and latent heat release near the typhoon center. The water vapor at 500 hPa in the CMA-TRAMS's simulation had become saturated, but the saturated area was much smaller than the analysis field, this may indicate the underdevelopment in size of the simulated typhoon. Above all, the ECMWF's forecast was limited by moisture condition so that failed to predict the generation of Noul. Meanwhile, the CMA-TRAMS indicated an over-forecast bias of Noul's intensity due to saturated moisture.

The pseudo-equivalent potential temperature represents the internal energy of the humid air, the higher the pseudo-equivalent potential temperature of the typhoon warm core is, the greater the internal energy of the air mass in the region. The air mass with larger internal energy, higher temperature, and lower density compared with surrounding air will surely produce violent upward motion, that is, convective instability [31-33]. As the typhoon grows stronger, the warmer core becomes more significant. As a result, the vertical distribution of the pseudo-equivalent potential temperature can not only reflect the stability of the atmosphere and the energy transport in different levels of the typhoon, but its shape can also demonstrate the columnar structure and the evolution process of the typhoon. During the early stage of typhoon genesis, the warm core structure is not obvious, but there are still some warm core characteristics. Both the analysis and the CMA-TRAMS simulation indicated these characteristics, as depicted in the following figure. Fig. 8 shows the vertical profile of the pseudo-equivalent potential temperature. As can be seen from the figure, both the analysis and CMA-TRAMS simulation clearly reflected the warm core structure of the typhoon, with a high-value zone in the cyclone center region, owing to the upward transport of both sensible and latent heat induced by the sea-land interaction. This, in turn, led to a relatively high distribution in the boundary layer. Meanwhile, in the middle troposphere of the high-value region, a relatively low-value region appeared near 600 hPa of the typhoon area. This was attributed to the fact that the sinking airflow in the central area of the cyclone became significantly drier while warming.

The distribution of vertical vorticity can be described as a reflection of the development of the disturbance, where the vorticity is high where the disturbance is strong and vice versa. Fig. 9 shows the vorticity at the lower and middle levels. In the analysis field, there was a positive vorticity column within a radius of 200 km around the

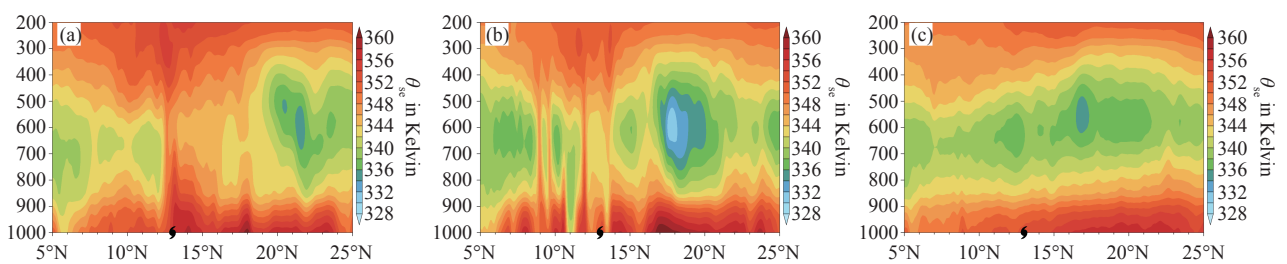

Figure 8. Pressure-latitude cross-section of pseudo-equivalent potential temperature (K; shading) from the (a) analysis data, (b) CMA-TRAMS forecast result initialized at 0000 UTC 12 September, and (c) ECMWF forecast result initialized at 0000 UTC 12 September.

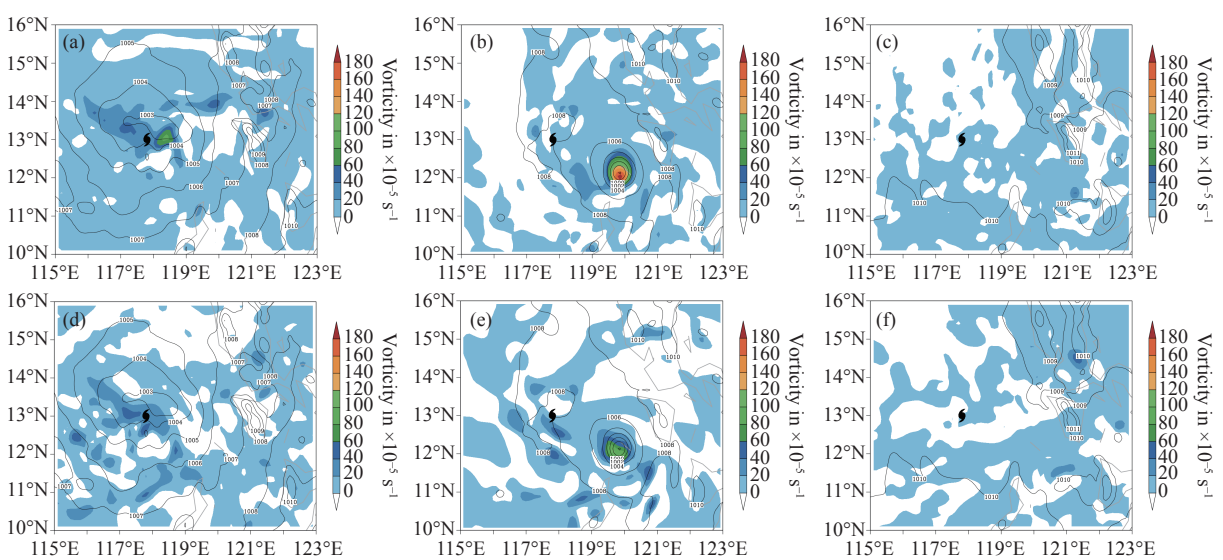

Figure 9. The vorticity from the (a, d) analysis field at 0000 UTC 16 September, (b, e) CMA-TRAMS forecast results initialized at 0000 UTC 12 September, and (c, f) ECMWF forecast results initialized at 0000 UTC 12 September. (a, b, c) present vorticity at 850 hPa, and (d, e, f) at 500 hPa.

typhoon, and the most significant positive vorticity zone was on the east of the typhoon. The maximum positive vorticity center lied in the lower troposphere, and the positive vorticity column extended upward above 500 hPa. The CMA-TRAMS also predicted a strong positive vorticity center at 850 hPa; however, there is a notable difference between the analysis and CMA-TRAMS, in the forecast field, the region of positive vorticity was smaller yet stronger, and located almost at the centre of the typhoon. At 500 hPa height, the intensity of the positive vorticity remained stronger than that of the analysis field. The dynamic term of higher positive vorticity in the lower troposphere significantly contributed to cyclogenesis. Overforecasting the dynamical factor of the CMA-TRAMS resulted in the fact that the typhoon's circulation structure and moving speed were not well predicted. Meanwhile, this missed forecast of Noul by the ECMWF might possibly be due to the inadequate forecast in terms of dynamic factor.

4 CONCLUSION

The CMA-TRAMS has updated to version 3.0 in 2019, with a resolution of 9 km, covering the western North Pacific and South China Sea regions and providing forecasts four times a day. The new version was evaluated here to assess the ability of cyclogenesis forecast. This study provided preliminary objective criteria based on typhoon observation data over the past five years and previous research, and the forecast results of the CMA-TRAMS in 2020 were evaluated from the perspective of cyclogenesis forecast. According to the statistical analysis, the CMA-TRAMS forecasted all TCs in its domain in 2020 at least 24 h in advance, while the ECMWF missed Hagupit (2004) and Goni (2019). Both the CMA-TRAMS and ECMWF had a maximum forecast lead time of 144 h for the genesis of Krovanh (2023). The CMA-TRAMS also forecasts the genesis of five other typhoons 144 h in advance. 82% of typhoons could be forecasted three days in advance by the CMA-TRAMS, while only 36% by ECMWF. The genesis position forecast errors of the CMA-TRAMS were 218.3 km, 158.13 km, and 99.84 km at lead times of 72, 48, and 24 h respectively. Combined with the objective verification results of 23 named TCs in 2020, the CMA-TRAMS genesis position forecast error at 72 h was comparable to the mean track error of both global and regional models. The model′s capability to predict TC genesis was demonstrated by these findings, and its forecast results could be used by forecasters to better understand the development of typhoons. The genesis forecast of Noul (2011) was briefly investigated. The 96 h forecast field of CMA-TRAMS had displayed a relatively organized three-dimensional structure of the typhoon.

Overall, the results suggested that the CMA-TRAMS has an advantage in cyclogenesis forecasts, but this research is still at a preliminary stage. Further work should include 1) expanding the sample dataset to the latest 10 years, and conducting experiments to update a set of more reasonable cyclogenesis criteria; 2) conducting a more detailed categorization of model-simulated cyclogenesis, early/late alarm and false alarm should be evaluated as well. Finally, evaluation work should be combined with mechanism analysis, to determine whether particular synoptic situations or model configurations are associated with model performance.

REFERENCES

[1] TANG B H, FANG J, BENTLEY A, et al. Recent advances in research on tropical cyclogenesis [J]. Tropical Cyclone Research and Review, 2020, 9(2): 87–105, https://doi.org/10.1016/j.tcrr.2020.04.004

[2] ZHANG Q H, GUO C R. Overview of the studies on tropical cyclone genesis [J]. Haiyang Xuebao, 2008, 30(4): 1–11, https://doi.org/10.3321/j.issn:0253–4193.2008.04.001, in Chinese with English abstract

[3] CHARNEY J C, ELIASSEN A. On the growth of the hurricane depression [J]. Journal of the Atmospheric Sciences, 1964, 21(1): 68–75, https://doi.org/10.1175/1520–0469(1964)0212.0.CO;2

[4] EMANUEL, KERRY A. An air-Sea interaction theory for tropical cyclones, Part I: Steady-state maintenance [J]. Journal of the Atmospheric Sciences, 1985, 43(6): 585–605, https://doi.org/10.1175/1520–0469(1986)0432.0.CO;2

[5] MONTGOMERY M T, ENAGONIO J. Tropical cyclogenesis via convectively forced vortex rossby waves in a Three-Dimensional Quasigeostrophic Model [J]. Journal of the Atmospheric Sciences, 1998, 55(20): 3176–3207, https://doi.org/10.1175/1520–0469(1998)0552.0.CO;2

[6] MONTGOMERY M T, NICHOLLS M E, CRAM T A, et al. A vortical hot tower route to tropical cyclogenesis [J]. Journal of the Atmospheric Sciences, 2006, 63(1): 355–386, https://doi.org/10.1175/JAS3604.1

[7] RITCHIE E A, HOLLAND G J. Scale interactions during the formation of Typhoon Irving [J]. Monthly Weather Review, 1997, 125(7): 1377–1396, https://doi.org/10.1175/1520–0493(1997)125<1377:SIDTFO>2.0.CO;2

[8] SIMPSON J, RITCHIE E, HOLLAND J G, et al. Mesoscale interactions in tropical cyclone genesis [J]. Monthly Weather Review, 1997, 125(10): 2643–2661, https://doi.org/ 10.1175/1520–0493(1997)125<2643:MIITCG>2.0.CO;2

[9] DUNKERTON T J, MONTGOMERY M T, WANG Z. Tropical cyclogenesis in a tropical wave critical layer: easterly waves [J]. Atmospheric Chemistry & Physics Discussions, 2008, 8(15): 5587–5646, https://doi.org/10.5194/acpd-8–11149–2008

[10] HALPERIN D J, FUELBERG H E, HART R E. An evaluation of tropical cyclone genesis forecasts from global numerical models [J]. Weather & Forecasting, 2013, 28(6): 1423–1445, https://doi.org/10.1175/WAF-D-13–00008.1

[11] YAMAGUCHI, MUNEHIKO, ISHIDA, et al. WGNE intercomparison of tropical cyclone forecasts by operational NWP models: A quarter century and beyond [J]. Bulletin of the American Meteorological Society, 2017, 98(11): 2337–2350, https://doi.org/10.1175/BAMS-D-16–0133.1

[12] CHEN J H, LIN S J, ZHOU L J, et al. Evaluation of tropical cyclone forecasts in the next generation global prediction system [J]. Monthly weather review, 2019, 147(9): 3409–3428, https://doi.org/10.1175/MWR-D-18–0227.1

[13] CHEN Guo-min, HUI Yu, QING Cao. Evaluation of tropical cyclone forecasts from operational global models over the Western North Pacific in 2013 [J]. Tropical Cyclone Research and Review, 2015, 4(1): 18–26, https://doi.org/ https://doi.org/10.6057/2015TCRR01.03

[14] DAS A K, RAMA RAO Y V, TALLAPRAGADA V, et al. Evaluation of the Hurricane Weather Research and Forecasting (HWRF) model for tropical cyclone forecasts over the North Indian Ocean (NIO) [J]. Natural Hazards, 2015, 75(2): 1205–1221, https://doi.org/10.1007/s11069–014–1362–6

[15] CHEN Guo-min, ZHANG Xi-ping, YANG Meng-qi, et al. Verification on forecasts of typhoons over western North Pacific and South China Sea in 2019 [J]. Meteorological Monthly, 2021, 47(10): 1266–1276, https://doi.org/10.7519/j.issn.1000–0526.2021.10.009, in Chinese with English abstract

[16] CHEN Guo-min, YANG Meng-qi, ZHANG Xi-ping, et al. Verification on forecasts of typhoons over western North Pacific and South China Sea in 2020 [J]. Meteorological Monthly, 2022, 48(4): 516–525, https://doi.org/10.7519/j.issn.1000–0526.2022.022101, in Chinese with English abstract

[17] PASCH R J, HARR P A, AVILA L A, et al. An Evaluation and Comparison of Predictions of Tropical Cyclogenesis by Three Global Forecast Models [Z]. Miami: NOAA/NWS/NCEP/TPC, 2006.

[18] HALPERIN D J, PENNY A B, HART R E. A comparison of tropical cyclone genesis forecast verification from three Global Forecast System (GFS) operational configurations [J]. Weather and Forecasting, 2020, 35(5): 1801–1815, https://doi.org/10.1175/WAF-D-20–0043.1

[19] HALPERIN D J, FUELBERG H E, HART R E, et al. Verification of tropical cyclone genesis forecasts from global numerical models: Comparisons between the North Atlantic and Eastern North Pacific Basins [J]. Weather and Forecasting, 2016, 31(3): 947–955, https://doi.org/10.1175/WAF-D-15–0157.1

[20] CHEN Lian-shou, DING Yi-hui. Introductory Summary on West Pacific Typhoons [M]. Beijing: Science Press, 1979: 10–11 (in Chinese).

[21] ZHANG Wen-long, CUI Xiao-peng. Review of the studies on tropical cyclone genesis, 2013, 29(2): 337–346, https://doi.org/10.3969/j.issn.1004–4965.2013.02.019, in Chinese with English abstract

[22] CHEN De-hui, XUE Ji-shan, YANG Xue-sheng, et al. New generation of multi-scale NWP system (GRAPES): general scientific design [J]. Science Bulletin, 2008, 53(22): 3433–3445, https://doi.org/10.1007/s11434–008–0494-z, in Chinese with English abstract

[23] CHEN Zi-tong, DAI Guang-feng, ZHONG Shui-xin, et al. Technical features and prediction performance of typhoon model for the South China Sea [J]. Journal of Tropical Meteorology, 2016, 32(6): 831-840, https://doi.org/10.16032/j.issn.1004–4965.2016.06.005, in Chinese with English abstract

[24] CHEN Zi-tong, XU Dao-sheng, DAI Guang-feng, et al. Technical scheme and operational system of tropical high-resolution model (TRAMS-V3.0) [J]. Journal of Tropical Meteorology, 2020, 36(4): 444–454, https://doi.org/10.16032/j.issn.1004–4965.2020.041, in Chinese with English abstract

[25] XU Dao-sheng, CHEN Zi-tong, ZHANG Yan-xia, et al. Updates in TRAMS 3.0 model version and its verification on typhoon forecast [J]. Meteorological Monthly, 2020, 46(11): 1474–1484, https://doi.org/10.7519/j.issn.1000–0526.2020.11.008, in Chinese with English abstract

[26] ECMWF. 2016: ECMWF IFS documentation [Z]. ECMWF, 2016. [Available online at http://www.ecmwf.int/en/forecasts/documentation-and-support/changes-ecmwf-model/ifs-documentation]

[27] GRAY W M. Tropical Cyclone Genesis in the Western North Pacific [R]. California: Naval Post-graduate School, 1975.

[28] LIANG Jia-hao, CHEN Ke-yi, LI Shu. The impact of different cumulus parameterization schemes of the WRF model on the Typhoon “Ryan” simulation over the South China Sea[J]. Journal of Chengdu University of Information Technology, 2019, 34(2): 162–171, https://doi.org/10.16836/j.cnki.jcuit.2019.02.010, in Chinese with English abstract

[29] JIANG Di, HUANG Fei, HAO Guang-hua, et al. The characteristics of air-sea heat flux exchange during the generation and development of local typhoon over the South China Sea[J]. Journal of Tropical Meteorology, 2012, 28(6): 888–896, https://doi.org/10.3969/j.issn.1004–4965.2012.06.010, in Chinese with English abstract

[30] KAPLAN J, DEMARIA M. Large-Scale characteristics of rapidly intensifying tropical cyclones in the North Atlantic Basin [J]. Weather and Forecasting, 2003, 18(6): 1093–1108, https://doi.org/10.1175/1520–0434(2003)0182.0.CO;2

[31] CIONE J J, UHLHORN E W. Sea surface temperature variability in hurricanes: implications with respect to intensity change [J]. Monthly Weather Review, 2003, 131(8): 1783–1796, https://doi.org/10.1175//2562.1

[32] ZHU T, ZHANG D L. The impact of the storm-induced SST cooling on hurricane intensity [J]. Advances in Atmospheric Sciences, 2006, 23(1): 14–22, https://doi.org/10.1007/s00376-006-0002-9

[33] LI M, HE Y, LIU G. Atmospheric and oceanic responses to Super Typhoon Mangkhut in the South China Sea: a coupled CROCO-WRF simulation [J]. Journal of Oceanology and Limnology, 2023, 41(4): 1369–1388, https://doi.org/10.1007/s00343-022-1328-6

Citation: LI Meng-jie, CHEN Zi-tong, DAI Guang-feng, et al. An Evaluation of Tropical Cyclone Genesis Forecast over the Western North Pacific and the South China Sea from the CMA-TRAMS [J]. Journal of Tropical Meteorology, 2024, 30(1): 20-28, https://doi.org/10.3724/j.1006-8775.2024.003